Surface potential around potassium promoter atoms on Rh(111) measured with photoemission of adsorbed Xe, Kr, and Ar

T. V. W. Janssens
Institute of Physical and Theoretical Chemistry, University of Bonn, D-53115 Bonn, Germany
and Schuit Institute of Catalysis, Eindhoven University of Technology, 5600 MB Eindhoven, The Netherlands

G. R. Castro and K. Wandelt
Institute of Physical and Theoretical Chemistry, University of Bonn, D-53115 Bonn, Germany

J. W. Niemantsverdriet*
Schuit Institute of Catalysis, Eindhoven University of Technology, 5600 MB Eindhoven, The Netherlands
(Received 3 December 1993)

The effect of potassium promoter atoms on Rh(111) on the surface potential has been investigated with photoemission of adsorbed Xe, Kr, and Ar. By using probe atoms of different sizes, we have measured the variation of the surface potential in the vicinity of a potassium atom. The surface potentials have been probed on Rh(111) surfaces, covered with 2.7, 4.1, and 5.0 at. % potassium. At all these coverages, we find a decrease in potential close to the potassium atoms (<4 Å) on the order of 1–2 eV, which depends on the lateral distance from the potassium atom. Further away from the potassium atoms we find a nearly constant potential that is 0.4–1.0 V lower than on unpromoted Rh(111). This implies that all available adsorption sites on the promoted surface are affected by the presence of potassium. The measured potentials depend on the potassium coverage, indicating that the potentials result from a cumulative effect of all potassium atoms on the surface. The observed changes in surface potential agree well with the potential in a hexagonal network of dipoles, indicating that they are of electrostatic origin and do not require long-range changes in electronic structure.

I. INTRODUCTION

Potassium is a well known promoter for many catalysts, for example those used in the synthesis of ammonia[1] and the hydrogenation of CO.[2,3] The main function of the alkali metal in these reactions is to facilitate the dissociation of the reactants N_2 and CO, respectively.

Adsorption of small amounts of potassium on a metal surface leads to a strong decrease of the macroscopic work function, due to charge transfer from the alkali to the metal surface.[3–9] A theoretical calculation of a single potassium atom on a semi-infinite jellium surface by Lang, Holloway, and Nørskov[10] shows that the electrostatic potential is lowered at adsorption sites directly adjacent to the potassium atom. This promotes the transfer of electron density from the metal to adsorbate molecules, which results in a stabilization of electron accepting adsorbates (e.g., CO and N_2) on the promoted sites of the surface,[11] as well as a concomittant destabilization of the intramolecular bond. Several experimental[3,4] and theoretical[12] studies confirm this picture. Evidence that the promoting effect of potassium on metal surfaces is predominantly a local one has been reported for various adsorbates and substrates.[3,7,8,13–20]

While techniques such as thermal desorption and electron and vibrational spectroscopy measure the effect of potassium in terms of altered properties of the adsorbate, photoemission of physisorbed noble gases enables one to monitor the electrostatic potential at different locations on the promoted surface. The measurement is based on the experimental observation that the binding energy with respect to the vacuum level, E_B^V, of Xe $5p_{1/2}$ electrons in Xe adsorbed on many different substrates falls within the range 12.3 ± 0.15 eV, and is thus practically independent of the substrate.[21,22] In ultraviolet photoemission spectroscopy (UPS), however, one measures binding energies with respect to the Fermi level of the substrate, E_B^F, which differs from E_B^V by the work function of the adsorption site, referred to as the local work function. As variations in the local surface potential correspond to variations in the local work function, photoemission of adsorbed Xe provides a way to measure the surface potential. The validity of this method is also supported by calculations of the ionization energy of Xe adsorbed on K/Rh clusters.[23] Of course, the values found represent an average over the volume of the Xe $5p_{1/2}$ orbital, which determines the spatial resolution of the measurement.

Markert and Wandelt applied photoemission of adsorbed xenon on potassium-promoted Ru(0001),[7,21] and found that the potential on Xe adsorption sites next to potassium is 0.57 eV lower than on sites further away.

In this paper, we use noble gases of different size—xenon, krypton, and argon—thus varying the lateral distance between the noble gas probe atoms and the potassium atoms. This allows one to investigate the variation of the surface potential around a potassium atom on Rh(111). In addition to the expected short-range de-

crease of the potential around the potassium we find a smaller, but significant long-range decrease of the surface potential, which we attribute to the cumulative contribution of all potassium atoms on the surface. In addition, we present theoretical calculations, which indicate that both long- and short-range effects of potassium that we measured are described adequately by the electrostatic effect of dipoles without the need to consider long-range changes in electronic structure of the substrate. A brief preliminary communication emphasizing the importance of this work for catalysis has appeared recently.[24]

II. EXPERIMENT

The experiments were done in an UHV system with a base pressure of 10^{-10} Torr, equipped with Auger-electron spectroscopy (AES), low-energy electron diffraction (LEED), UPS, and a mass spectrometer. The Rh crystal with a [111]-oriented surface was mounted on a sample holder by tungsten wires pressed into grooves in the side faces of the crystal, which allowed the sample to be heated resistively up to 1300 K. The sample holder was connected via a copper string to a He refrigerator, allowing cooling of the sample to 45 K.[25] The temperature has been measured by a NiCr-Ni thermocouple spotwelded to the back of the crystal. The cleaning procedure entailed cycles of Ar bombardment (1 keV, 1.5 μA sample current), heating in oxygen (10^{-7} Torr) at 900 K and flashing into vacuum to 1250 K. To maintain the cleanliness of the sample, the heating in oxygen and flashing was repeated daily.

Potassium-covered surfaces were prepared by depositing a few layers of potassium on the surface at $\sim$50 K, using a commercial getter source (SAES), and subsequent heating at $\sim$2 K/s to a final annealing temperature between 700 and 850 K, at which the sample was kept for 1 min. Preparations at 845, 755, and 710 K resulted reproducibly in coverages of 2.7, 4.1, and 5.0 at. %, respectively (1 at. % = 1 K atom per 100 Rh surface atoms), as estimated from the adsorption geometry of noble gas atoms on these surfaces, which we discuss below. At all these coverages the potassium is ionic.[4,6]

At each potassium coverage we adsorbed noble gases in small incremental doses at 45 K, while HeI–UPS spectra were recorded after each adsorption step. After completion of a series with one noble gas, the latter as well as contaminating CO or water were desorbed by a short flash to 600 K, and the measurements were continued with the next noble gas. This procedure ensures a clean surface and a constant potassium coverage in one series of experiments with Xe, Kr, and Ar, which has been confirmed by the reproducible work function of the potassium-covered surface before each experiment (4.4 eV for $\theta_K = 2.7$ at. %, 3.7 eV for $\theta_K = 4.1$ at. %, and 3.1 eV for $\theta_K = 5.0$ at. %).

UPS spectra of the adsorbed noble gases were decomposed by fitting them with linear combinations of measured or calculated base spectra, as described elsewhere.[26] For a single Xe state, two Gauss-Lorentz curves, as described by Fraser and Suzuki,[27] have been used, corresponding to $5p_{1/2}$ and $5p_{3/2}$, respectively. The analytical form of these curves contains a parameter a, which allows a smooth change of the shape from purely Gaussian ($a=0$) to purely Lorentzian ($a=1$). In the decompositions presented here, this parameter is fixed to $a = 1/\sqrt{2}$. We allow intensity, width, and position to change. The separation of the Xe $5p_{1/2}$ and $5p_{3/2}$ peaks has been kept at 1.3 eV; their intensity ratio lies between 1.0 and 1.5.

Making physically meaningful fits of the Kr and Ar spectra using the Gauss-Lorentz curves is difficult, due to overlap of the spin-orbit split signals, which leads to numerical problems. Therefore, we have used measured Kr and Ar spectra, representing a single adsorption state, as base functions for the fits. This guarantees a correct separation between spin-orbit states with the correct intensity ratio.

III. RESULTS

We will first discuss the UPS spectra of Xe, Kr, and Ar on clean Rh(111), and check whether interpretation of the Kr and Ar binding energies in terms of local work functions, similarly as for Xe, is permitted. Next we present the spectra of Xe, Kr, and Ar adsorbed on potassium-covered Rh(111) with three different loadings of potassium. Finally, we discuss adsorption geometries of the noble gases on the three K/Rh(111) surfaces, from which the potassium coverage and the distances between the noble gases and the potassium atoms are evaluated.

A. Adsorption of Xe, Kr, and Ar on clean Rh(111)

Figure 1 shows the HeI–UPS spectra of Xe, Kr, and Ar adsorbed on clean Rh(111), after subtraction of the Rh background. The Xe $5p$ and Kr $4p$ spectra are spin-orbit doublets, with splittings of 1.3 and 0.67 eV, respectively, which are equal to the gas phase values.[28] The splitting of the $3p$ signal for gaseous Ar is 0.18 eV,[28] which remains unresolved in the UPS spectrum for adsorbed Ar. The uniform signals of the adsorbed noble gases at low coverages indicate that the Rh(111) surface is homogeneous and mostly defect free. After a certain exposure of Xe or Kr new peaks appear, accompanied by the attenuation of the original signal. This is characteristic of the formation of the second and higher layers. With Ar, multiple layers are formed at Ar pressures above 10^{-5} Torr at 45 K.

Physisorbed krypton and argon can only be used as probes for the surface potential if their ionization energy with respect to the vacuum level is independent of the substrate, as is the case with xenon. The crucial test is to check whether on homogeneous, flat surfaces—where the *local* work function equals the *macroscopic* work function—the binding energy with respect to the Fermi level, E_B^F, and the work function φ add up to a constant value equal to E_B^V.[21,22] The work function of the Rh(111) surface, determined from the width of the HeI–UPS spectrum, is 5.60 eV.[6,9] Table I gives relevant data for adsorption of Xe, Kr, and Ar on Rh(111) as well as on other surfaces. Unfortunately, only a few binding energies of adsorbed Kr and Ar have been reported.[29–31] Nevertheless, the values that are available indicate that

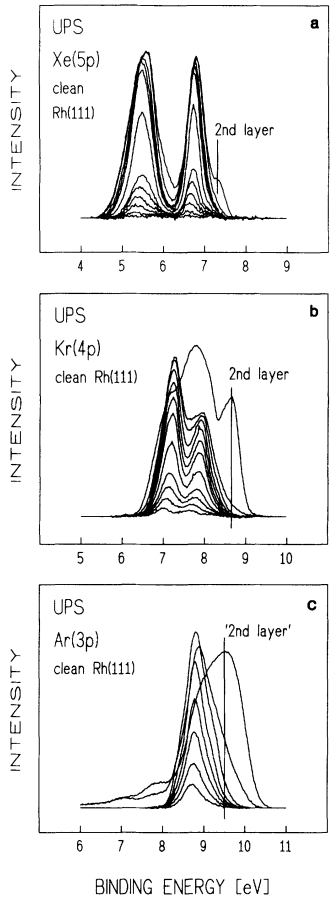

FIG. 1. HeI–UPS spectra of (a) Xe, (b) Kr, and (c) Ar on clean Rh(111) adsorbed at 45 K. The uniform signals for adsorbed noble gases in the first layer indicate a homogeneous surface potential.

the ionization energy of adsorbed Kr and Ar does not depend on the substrate. We will therefore interpret a shift of the binding energy of adsorbed Kr and Ar in UPS as a change in the local surface potential, similarly as for Xe.

The last two columns of Table I show that the ionization energy of the adsorbed noble gases is lower than in the gas phase,[28] due to the extra-atomic relaxation caused by the presence of the metal surface.[21,22] The extra-atomic relaxation energy is governed by the image potential. Hence it is larger for the smaller atoms, in agreement with our observation.

B. Adsorption of Xe, Kr, and Ar on K/Rh(111) surfaces

The left half of Fig. 2 shows the HeI–UPS spectra of Xe, Kr, and Ar adsorbed on Rh(111), precovered with 2.7 at. % potassium, after subtraction of the background of potassium-covered Rh. Compared to the spectra of the noble gases on clean Rh(111) (see Fig. 1), we see additional peaks for Xe, Kr, and Ar, which already develop after low exposures. This directly indicates a potassium-induced heterogeneity of the surface potential. The right half of Fig. 2 displays typical decompositions of Xe, Kr, and Ar spectra into contributions corresponding to different adsorption states.

The spectrum for a submonolayer of Xe, Kr, or Ar adsorbed on potassium-covered Rh(111) consists of two contributions, identified with adsorption on bare Rh sites (A) and adsorption on sites next to a potassium atom (B) (see Fig. 2). This assignment of the peaks is consistent with the intensities found at higher potassium loadings and with the assignment for Xe on potassium-covered Ru(0001).[7] Though not well visible in Fig. 2, the noble gases adsorb preferentially on the sites next to potassium, as can be derived from the relative intensities in

TABLE I. The binding energy with respect to the vacuum level, determined by addition of the work function of the Rh(111) surface and the binding energy in HeI–UPS, for Xe ($5p_{1/2}$), Kr ($4p_{1/2}$), and Ar ($3p$) adsorbed on clean Rh(111). The differences of these values from those of gaseous Xe, Kr, and Ar is the extra-atomic relaxation energy due to the presence of the Rh surface.

	E_B^F (eV) Rh(111)	$E_B^F+\varphi$ (eV) Rh(111)[a]	Other substrates		E_B^V (eV) Gas phase	Relaxation energy (eV)
Xe	6.7	12.3	12.3±0.15	25 substr.[b]	13.4[c]	1.1
Kr	7.7	13.3	13.3	$Cu_3Pt(111)$[d]	14.7[c]	1.4
Ar	8.7	14.3	14.3	Ni(100)[e]	14.8[c,f]	1.5
			14.4	Ru(001)[g]		
			14.4	Cu/Ru(001)[g]		

[a]Work function of Rh(111) is 5.60 eV.
[b]The 25 substrates include transition metals, alkali metals, Al, Si, and oxides (TiO_2 and ZnO); Refs. 21 and 22.
[c]Reference 28.
[d]Reference 29.
[e]Reference 30.
[f]Ar $3p_{3/2}$ level.
[g]Reference 31.

the spectra at low noble gas coverage. This indicates a higher adsorption energy for Xe, Kr, and Ar on these sites. In the case of Xe and Kr, peaks corresponding to adsorption on top of potassium (C) and formation of the second layer occur after high exposures; for Ar these states are only observed at Ar pressure above 10^{-6} Torr. At every potassium coverage studied, the adsorption sites are occupied in this order.

The decompositions of the spectra shown in the right half of Fig. 2 yield the binding energy of the noble gas signals and the distribution of the noble gas atoms over the different adsorption sites. The binding energies can be determined with good accuracy; the potassium-induced changes in binding energy E_B^F for Xe, Kr, and Ar are listed in Table II. A reliable quantitation of the available adsorption sites on the surface is obtained from the spectrum of a complete monolayer of adsorbed noble gas.

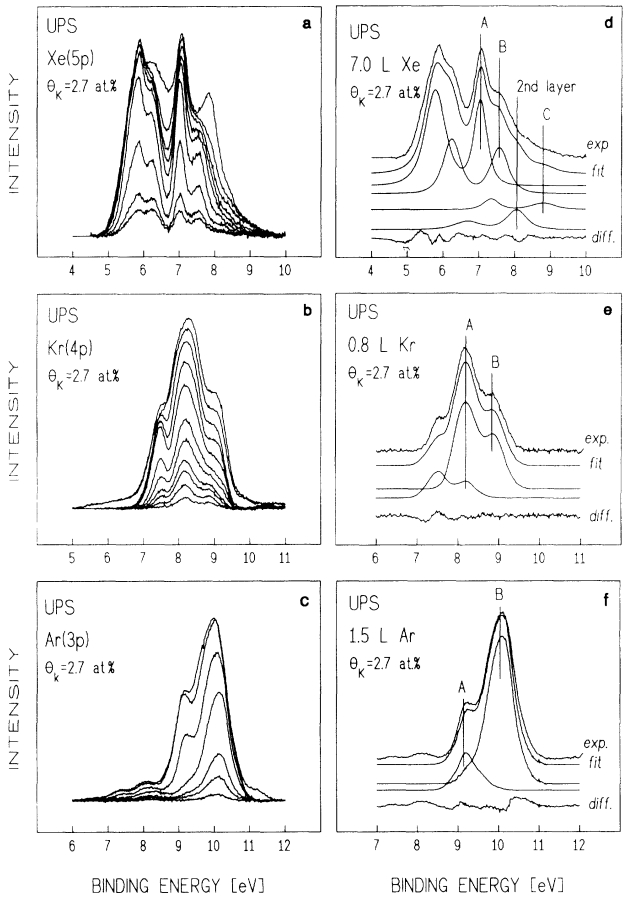

FIG. 2. Left part: HeI–UPS spectra of (a) Xe, (b) Kr, and (c) Ar adsorbed on potassium-covered Rh(111) (potassium coverage: 2.7 at. %). The K/Rh background has been subtracted. The effect of the potassium is a splitting of the noble gas spectrum into at least two contributions and a shift to higher binding energy. Right part: typical decompositions of (d) Xe, (e) Kr, and (f) Ar spectra into contributions corresponding to the different noble-gas adsorption sites on the surface: Rh sites (A), sites adjacent to potassium (B), and sites on top of potassium (C). The curve labeled (diff.) is the difference between the experimental (exp.) and fitted (fit.) curves.

Such data are only available for adsorbed Xe; for Kr and Ar, the onset of second-layer adsorption is detected before completion of the first layer on potassium-covered Rh(111), which interferes with the spectra for the first layer: the Kr and Ar atoms form three-dimensional clusters around the potassium atoms, because of weak Kr and Ar bonding to the surface. Since the positions of the peaks related to Kr and Ar in the first layer have been determined from the spectra at low noble gas coverages, which are not disturbed, this is of no consequence for the binding energy E_B^F nor the potassium coverage, which is derived from these measurements (see Sec. III C). In the spectrum of a Xe monolayer on the 2.7% K/Rh(111) surface, we find that 52% of the intensity corresponds to Xe on Rh sites (A), 40% to Xe on sites adjacent to potassium (B), and 8% to Xe on top of potassium (C). As we will show in Sec. III C, this distribution of the Xe atoms over the different adsorption sites corresponds to a potassium coverage of 2.7 at. %.

Figures 3(a) and 3(b) show the background-subtracted HeI–UPS spectra of Xe and Kr on Rh(111), precovered with 4.1 at. % potassium. Spectra of Ar adsorption on this surface were not measured. The right-hand side of Fig. 3 shows a characteristic decomposition of Xe and Kr spectra.

Similarly as for spectra at $\theta_K = 2.7$ at. %, the spectra of Xe and Kr at low coverages on Rh(111) precovered with 4.1 at. % potassium consist of two contributions, assigned to adsorption on Rh sites (A) and sites next to potassium (B) (see Fig. 3). The changes in binding energy for these adsorption sites with respect to those of clean Rh(111) are listed in Table II. Compared to the surface with 2.7 at. % potassium, we find relatively more Xe on sites next to potassium, in agreement with the assignment of the peaks. The Kr UPS spectra of this surface are disturbed by the formation of a second Kr layer, which develops before the first layer is completed. The full monolayer of Xe consists of 16% Xe on Rh (A), 71% Xe on sites next to potassium (B), and 13% on top of potassium (C).

Figure 4 shows the HeI–UPS spectra for Xe, Kr, and Ar on Rh(111), precovered with 5 at. % potassium, and typical decompositions of the spectra in the contributions of the different adsorption states. Increasing the potassium coverage to 5 at. % leads to a further reduction of the available Rh sites for the noble gases. An interesting point is that in the spectra for Xe on this surface, the signal related to Xe on Rh sites has almost disappeared, whereas those for Kr and Ar on Rh sites are clearly visible, in agreement with their smaller size. The changes in binding energy, evaluated from the decompositions, are listed in Table II. In a complete monolayer of Xe on this surface, we find 5% adsorbed on Rh sites (A), 80% on sites next to potassium (B), and 15% on top of potassium (C).

C. Determination of the distances between potassium and noble-gas atoms

In this section, we estimate absolute potassium coverages as well as distances between potassium atoms and

TABLE II. Binding-energy shifts of the Xe $5p_{1/2}$, Kr $4p_{1/2}$, and Ar $3p$ signal in HeI–UPS, for the different adsorption sites on potassium-covered Rh(111) at different potassium coverages. The distances between the adsorption site and the potassium atoms have been calculated from a fivefold coordination of the noble gases around potassium, using the van der Waals radii of the noble gases (2.2 Å for Xe, 2.0 Å for Kr, and 1.9 Å for Ar) and the ionic radius of potassium (1.33 Å) (Ref. 32).

Adsorption site	Estimated distance to K (Å)	Binding-energy shift (eV) 2.7 at. %	4.1 at. %	5.0 at. %
next to K				
Ar	3.23	1.44		1.66
Kr	3.40	1.13	1.33	1.57
Xe	3.74	0.87	1.15	1.31
next nearest to K				
Ar	5.90	0.43		1.04
Kr	6.23	0.42	0.72	1.00
Xe	6.83	0.35	0.61	

noble gas atoms on the various adsorption sites. In order to do this, we construct adsorption geometries, shown in Fig. 5, for the potassium and Xe atoms on the surface, such that the distribution of Xe adsorption sites matches the distribution derived from the spectrum of a complete Xe monolayer [see Figs. 2(d), 3(c), and 4(d)]. The geometries for Kr and Ar are found by replacing the Xe atoms in the model for the smaller Kr and Ar atoms, leaving the potassium coverage constant (see Fig. 5). We

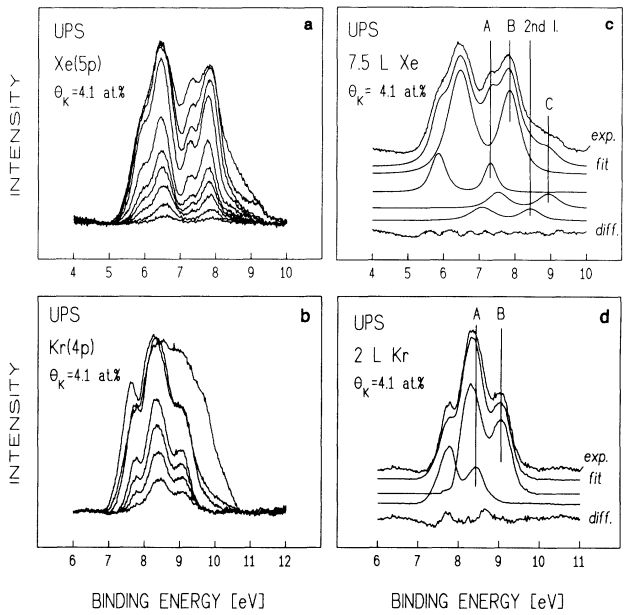

FIG. 3. Left part: HeI–UPS spectra of (a) Xe and (b) Kr adsorbed on potassium-covered Rh(111) (potassium coverage: 4.1 at. %). The K/Rh background has been subtracted. Right part: typical decompositions of (c) Xe and (d) Kr spectra into contributions corresponding to the different noble-gas adsorption sites on the surface: Rh sites (A), sites adjacent to potassium (B), and sites on top of potassium (C). The curve labeled (diff.) is the difference between the experimental (exp.) and fitted (fit.) curves.

expect that these adsorption geometries give realistic average potassium-potassium distances, from which the potassium coverage is determined, and noble-gas—potassium distances for adsorption on sites adjacent to potassium, and the distance of adsorbed noble gases on next-nearest-neighbor sites.

Due to the strong repulsion, the potassium is atomically dispersed at low coverages. For the adsorption geometries we assume that the potassium atoms form ordered structures of hexagonal symmetry, and we neglect the corrugation of the Rh surface. The size of the noble gas atoms is given by the van der Waals radii (2.2 Å for Xe, 2.0 Å for Kr, and 1.9 Å for Ar);[32] for potassium we take the ionic radius (1.33 Å).[32]

With 2.7 at. % potassium on Rh(111), the intensities of Xe on Rh sites (A), Xe on sites next to potassium (B), and Xe on top of potassium (C) are in the proportion of $A:B:C=6.5:5:1$. By placing the atoms, with sizes given above, on the surface, we can construct a unit cell, containing six Xe atoms on Rh sites, five Xe atoms next to potassium, and one potassium atom [see Fig. 5(a)]. Note that the unit cell allows continuation over the whole surface. Considering that the unit cell is an approximation which allows only an integer number of Xe atoms, this is an acceptable model to describe the surface. The distance between potassium atoms that results from this distribution of Xe atoms is 16.1 Å, which corresponds to 4.32×10^{13} potassium atoms per cm^2. Division by the number of Rh surface atoms per cm^2 (1.6×10^{15}) yields a potassium coverage of 2.7 at. %. The distance between the potassium atoms in the model should be interpreted as a mean distance on the surface. The ratio $B:C$ of 5 points to a fivefold coordination of Xe around potassium, which has also been found for Xe on potassium-covered Ru(0001).[7]

At $\theta_K=4.1$ at. %, the ratio of Xe on Rh sites (A), sites next to potassium (B), and sites on top of potassium is $A:B:C=1.2:5.6:1$ for a full Xe monolayer. The corresponding unit cell, shown in Fig. 5(b), has two Xe atoms on Rh sites, and five on sites next to potassium. The symmetry of the unit cell does not allow us to place one Xe

atom in a unit cell; we have to choose between zero and two. Since we have a considerable amount of Xe on Rh sites, we have chosen the option with two Xe atoms per unit cell. The mean distance between the potassium atoms is then 13.2 Å, corresponding to a potassium coverage of 4.1 at. %.

At $\theta_K = 5.0$ at. %, the ratio for Xe on Rh (A), Xe next to potassium (B), and Xe on top of potassium (C) is $A:B:C = 0.3:5.3:1$ in a complete monolayer. The unit cell corresponding to this distribution is shown in Fig. 5(c). In this unit cell we have five Xe atoms, all adsorbed on sites adjacent to potassium. The distance between the potassium atoms is 12.0 Å, which corresponds to a potassium coverage of 5.0 at. %. At this potassium density, there is sufficient space to set Kr and Ar on Rh sites, while this is not possible for Xe [see Fig. 5(c)]. This is in agreement with the spectra shown in Fig. 4, which indeed indicate that the intensity for Xe on Rh sites (A) is low. This feature makes the potassium density in Fig. 5(c) an acceptable one. The low but nonzero intensity for Xe on Rh at this potassium coverage [see Fig. 4(d)] is probably caused by a slightly inhomogeneous distribution of the potassium atoms over the surface, and corresponds to a locally lower potassium density. We omit it in the further interpretation.

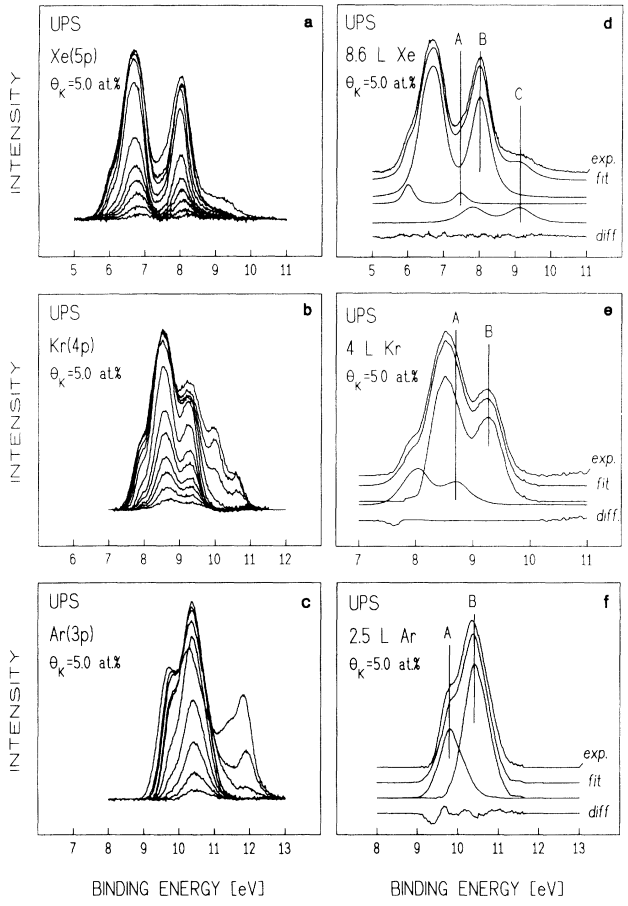

FIG. 4. Left part: HeI–UPS spectra of adsorbed Xe (a), Kr (b), and Ar (c) on potassium-covered Rh(111) (potassium coverage: 5.0 at. %). The K/Rh background has been subtracted. Contrary to the surfaces with 2.7 and 4.1 at. % potassium, the contribution of Xe on Rh is almost absent. Right part: typical decompositions of (d) Xe, (e) Kr, and (f) Ar spectra into contributions corresponding to the different noble gas adsorption sites on the surface: Rh sites (A), sites adjacent to potassium (B), and sites on top of potassium (C). The curve labeled (diff.) is the difference between the experimental (exp.) and fitted (fit.) curve.

All structure models in Fig. 5 point to a fivefold coordination of potassium by noble gases in the first coordination shell. We use this to calculate the distance between the potassium atom and the noble gas atoms. Figure 6 shows a potassium atom (K) with two noble gas atoms in the fivefold coordination position (B_1 and B_2), and a noble gas atom at the closest possible Rh site (A). The distance between the potassium and the neighboring noble gas atom (K-B_1) follows from

$$d = \frac{r}{\sin 36^\circ} = 1.701 \times r \ , \tag{1}$$

where r is the van der Waals radius of the adsorbed noble gas; the angle α is 36°. Due to the fivefold coordination, the distance between a potassium atom and the noble gas sites adjacent to potassium is somewhat larger than the sum of the radius of potassium and the van der Waals radius of the noble gas.

The shortest possible distance between a potassium atom and a Rh site is found by placing a third noble gas atom (A) in the hexagonal-closest-packed position to two noble gas atoms next to potassium (B_1 and B_2 in Fig. 6). Its distance ($KD + DA$) to the nearest potassium atom is then given by

$$d = \frac{r}{\tan 36^\circ} + 2 \times r \cos 30^\circ = 3.108 \times r \ . \tag{2}$$

Equations (1) and (2) provide an estimate of the distance between a potassium atom and the noble gas adsorption sites. The values for Xe, Kr, and Ar are listed in Table II, together with the corresponding binding-energy shifts for adsorption on these sites.

IV. DISCUSSION

A. Potassium-induced changes in local surface potential

As explained in Sec. I the shifts of the noble gas UPS signals can be interpreted as changes in local surface potential. The orbital-averaged potential, which is measured in the photoemission experiments, is in first-order approximation equal to the potential at the center of the noble gas atom. Then the symbols in Figs. 7 and 8 depict the experimentally determined changes in surface potential, due to the adsorbed potassium, as a function of the distance to the nearest potassium atom. Figure 7 shows the experimentally determined variation in surface potential between two potassium atoms along the edge of a unit cell as depicted in Fig. 5(a) at $\theta_K = 2.7$ at. %.

For all potassium coverages studied—2.7, 4.1, and 5.0 at. %—we find a steeply decreasing surface potential in the direct surroundings of the potassium atom (<4 Å)

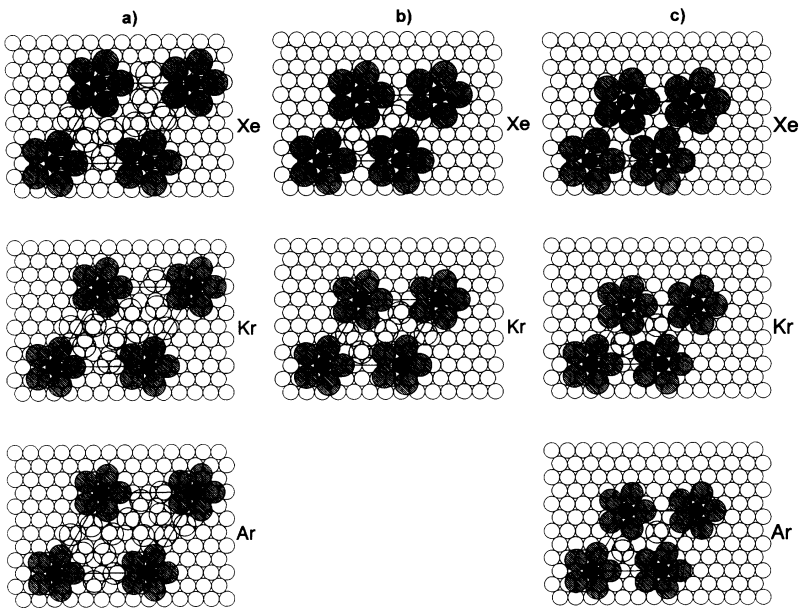

FIG. 5. Likely adsorption geometries for Xe, Kr, and Ar on potassium-covered Rh(111) at $\theta_K =$ (a) 2.7 at. % (K-K distance: 16.1 Å), (b) 4.1 at. % (K-K distance: 13.2 Å), and (c) 5.0 at. % K-K distance: 12.0 Å). Dark circles: potassium atoms. Hatched circles: noble gas atoms on the sites adjacent to potassium. Gray shaded circles: noble gas atoms on bare Rh sites.

and a smaller, but significant and practically constant, decrease in potential in all sites further away (> 5 Å). The symbols in Fig. 8 indicate that all sites available for noble gas adsorption on the surface—thus not only those close to potassium—are affected by the presence of potassium.

The measured potentials depend on the potassium coverage. However, this effect is larger at sites further away. It indicates an increased influence of the next-nearest potassium atoms at higher potassium loadings. The surface potential results from a cumulative effect of all potassium atoms on the surface.

To arrive at Fig. 8, we have used adsorption geometries constructed on the basis of the measured distribution of a complete monolayer of Xe over the different adsorption sites to estimate the lateral distance between potassium and noble gas atoms. Note, however, that these adsorption geometries are not at all critical. The distance between a potassium atom and its neighboring noble gas sites is approximately the sum of the radii of the potassi-

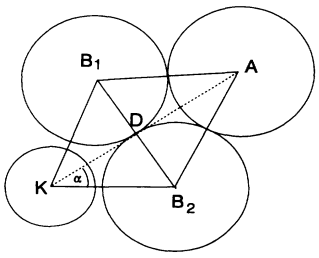

FIG. 6. Geometry used for determining the distance between potassium and noble gas atoms. K is the potassium atom, A is a noble gas atom at the bare Rh site that is closest to the potassium atom, and B_1 and B_2 are noble gas atoms at the sites next to potassium. Due to the fivefold coordination of the noble gas around potassium, the angle α is 36°.

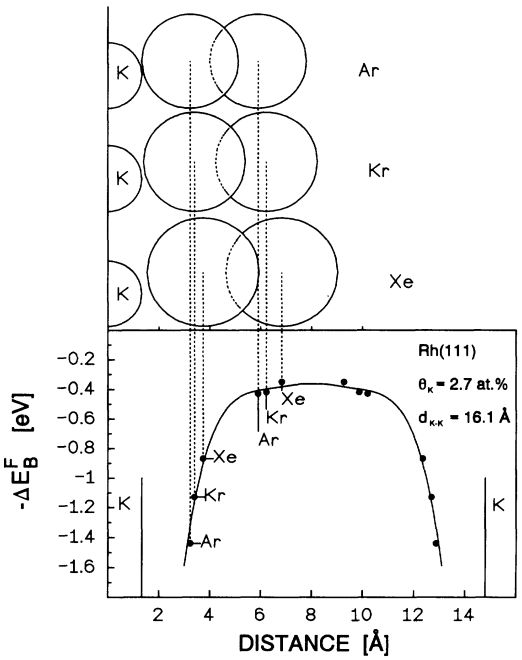

FIG. 7. Graphic representation of the measured shifts of the UPS signals of adsorbed Xe, Kr, and Ar on potassium-covered Rh(111) (θ_K=2.7 at. %), referenced to the UPS signals of adsorbed noble gas on clean Rh(111). These shifts are interpreted as the potassium-induced change in local surface potential along the edge of a unit cell as depicted in Fig. 5. The vertical lines indicate the size of the potassium ion. The solid line is drawn as a guide to the eye. A side view of the positions of the Xe, Kr, and Ar probe atoms with respect to the potassium atoms on the surface is also displayed. Close to a potassium atom we find a strong decrease in potential. Further away the potential is constant, but significantly lower than on clean Rh(111). Note that the potassium changes the potential at all available adsorption sites on the surface.

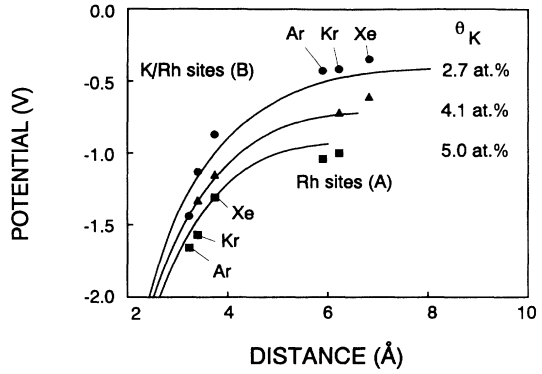

FIG. 8. Comparison of the experimentally determined potassium-induced changes in surface potential on Rh(111) at $\theta_K=2.7$, 4.1, and 5.0 at. % (symbols) with the electrostatic potential in a dipole network (solid lines) at 2.5 Å from the image plane, using a dipole moment of 10 D. The agreement between experimental and measured values indicates that the change in surface potential is due to the cumulative effect of all dipoles on the surface.

um and noble gas atoms, which also results from the fivefold coordination of the noble gas atoms around potassium. Figures 7 and 8 indicate that the variation in potential at the Rh sites further away from potassium remains within experimental accuracy limits: all these sites are equivalent with respect to the surface potential. Therefore, the exact distance between a noble gas atom at a Rh site and the nearest potassium is not important for the value of the potential.

The interpretation of the curves depicted in Fig. 8 as changes in local surface potential presuppose that the presence of potassium does not affect the extra-atomic relaxation energy of the adsorbed noble gases. The extra-atomic relaxation energy for adsorbed noble gases on a metal surface is determined by the image potential, which depends on the distance between the noble gas atom and metal surface. Since this distance does not change upon potassium adsorption, we do not expect a substantial change in the extra-atomic relaxation energy due to the presence of potassium on the surface.

B. Electrostatic model for the observed changes in potential

In this section, we show that the observed changes in surface potential are predominantly of electrostatic origin. We describe the potassium-covered Rh surface with an infinite, hexagonally ordered network of dipoles. Each dipole contains positive and negative point charges placed symmetrically at given distances from the image plane. This represents a positively charged potassium atom and its image charge in the metal surface. The potassium-induced changes in the surface potential correspond to the potential in the network. The potential at a given point (x,y,z) is calculated by adding the contributions of the dipoles separately:

$$V(x,y,z)=\frac{Qe}{4\pi\varepsilon}\sum_{(p,q)\in P}\left[\frac{1}{R_{\text{neg}}}-\frac{1}{R_{\text{pos}}}\right], \tag{3}$$

where Q is the nominal charge, e is the elementary charge (1.6×10^{-19} C), ε is the dielectric constant, and P is the set containing the position of the dipoles in the image plane. R_{neg} and R_{pos} are the distances between the point (x,y,z) and the position of the negative and positive charges of a dipole, respectively. These parameters include both the dipole length, which, together with the point charge value, determines the dipole moment, and the lateral distance between the dipoles. The latter corresponds to the potassium coverage.

The solid lines in Fig. 8 are calculated potentials in the network of dipoles, as a function of the distance to the nearest dipole at 2.5 Å from the image plane. The lateral distances between the dipoles have been taken from Fig. 5; the dipole moment used is 10 D, in the same order of magnitude as the experimental value for potassium adsorbed on Rh(111) ($\mu^0=7.8\pm0.5$ D for $\theta_K<5$ at. %), evaluated from work-function measurements using the Helmholtz equation.[8] Since the experimental value of the dipole moment of potassium at coverages below 5 at. % is constant within the limits of accuracy, we believe that the K-K depolarization can be ignored. Another assumption is that the effect of the polarized noble gas atoms on the probed potential is small. The semiquantitative agreement between measured and calculated values (see Fig. 8) indicate that the observed changes in surface potential can to first approximation be understood from the electrostatic potential in a network of dipoles, without the need to invoke major long-range changes in electronic structure.

Representing the potassium-covered Rh surface by dipoles consisting of point charges is the simplest conceivable approach. In order to investigate the effect of the distance between the charges of the dipole and the effect of distributing the negative charge over a larger area, we have performed the calculations reported in Table III. In practice, the potential at distances larger than 3 Å from a dipole depends mainly on the value of the dipole moment, irrespective of the exact positions of the point charges. Increasing the dipole length from 2 to 4 Å results in a 0.13-V lower potential at the potassium-promoted sites (Table III), a change of about 10%. The potential at the Rh sites is nearly unaffected. Assuming that the positive charge is located at the center of the potassium atoms, and the negative charge in the first Rh layer, we estimate a dipole length of 2.18 Å for potassium on a threefold site, and 2.67 Å for potassium on top of a Rh atom. Thus the consequence of the uncertainty of the positions of the point charges on the calculated potentials is limited to ~0.1 eV at most.

The image charge model is valid at large distances from the charges in the surface. The real charge distribution in the surface, however, is not point-charge-like[33,34] and may affect the potential close to the potassium ions. To estimate the possible effects of such a charge distribution on the potential at the adsorption site of the noble gas probe atoms, we have split the negative charge into several (N) charges with a charge value Q/N, which are distributed symmetrically over a circle around the image position parallel to the image plane. The effect of the number of negative charges appears to be negligible

TABLE III. Calculated potentials in the dipole network at 2.5 Å from the image plane for a dipole moment of 10 D at a K/Rh site (3.2 Å from a dipole) and a Rh site (6.4 Å from a dipole) for different charge distributions. Parameters are the number of negative charges, the radius of the circle at which the negative charges are placed (r_{neg}) and the dipole length.

Number of negative charges	Radius r_{neg} (Å)	Dipole length (Å)	Potential at the K/Rh site (V)	Potential at the Rh site (V)
1[a]		2	−1.27	−0.47
3[b]	1.0		−1.28	−0.45
6	1.0		−1.29	−0.45
60	1.0		−1.29	−0.45
3[b]	2.5	2	−1.32	−0.36
1[a]		4	−1.14	−0.45
3[b]	1.0		−1.15	−0.44
3[b]	2.5		−1.18	−0.41

[a]Dipole
[b]Distributed negative charge

(Table III); changing the radius of the circle, however, has a larger effect. At positions close to the negative charge, i.e., close to the surface and close to a dipole, the potential is strongly affected by the charge distribution. However, at the positions relevant for Fig. 8, the error in the potential due to the charge distribution is of the order of 0.05–0.1 V (Table III). In conclusion, the potential at the noble gas adsorption sites is determined mainly by the dipole moment alone; the position and distribution of the charges do not affect the calculated potential significantly.

An estimate for the error made by attributing the UPS peak shift to the potential at the center of the probe atom is obtained from the average potential over the volume of the probe atom, which can be calculated with the dipole model. Using a dipole moment of 10 D, which matches the measured potentials, we find that the averaged potential is ~10% lower than the potential at the position of the center of a probe atom next to potassium; for the probe atoms on the bare Rh sites the deviation is ~2%.

Figure 9 shows the electrostatic potential in front of the image plane of the network of dipoles (dipole moment 10 D, dipole length 2 Å, distance between dipoles 16.1 Å, corresponding to a potassium coverage of 2.7 at. %). Above 15 Å from the image plane, the potential hardly depends on the position with respect to the dipoles: The potential is virtually homogeneous and its value with respect to that of clean Rh(111) corresponds to the macroscopic work function decrease. At 15 Å above the surface, the lateral electrostatic field, which is a measure for the heterogeneity of the potential, is more than 1000 times smaller than the lateral field close to the surface. This means that adsorbates sense the position of the potassium promoter atoms only when they are close, i.e., within ~10 Å, to the surface. The heterogeneous surface potential that we have measured only exists close to the surface.

Figure 10 displays the potential in the network of dipoles in a plane 2.5 Å above the image plane for 2.7 at. % potassium coverage and a dipole moment of 10 D. Close to each potassium atom, the potential is strongly lowered, mainly due to the influence of the nearest potassium atom only. Further away the potential merges into a virtually constant value, which is still lower than on unpromoted Rh, determined by the cumulative effect of all potassium atoms on the surface. This picture reflects the

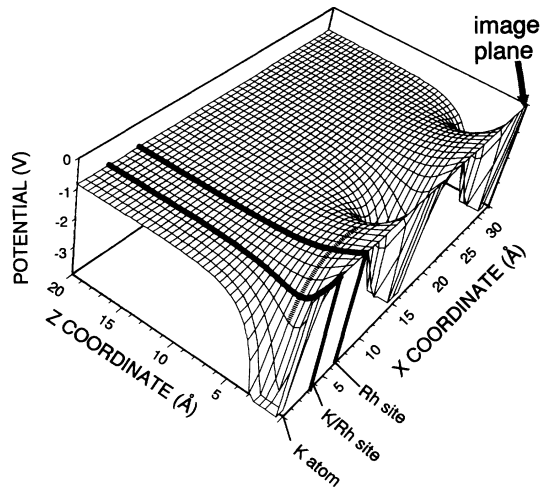

FIG. 9. Three-dimensional representation of the electrostatic potential perpendicular to the image plane in a hexagonally ordered network of dipoles. The point charges have been placed at 1 Å from the image plane; the dipole moment is 10 D. The distance between the dipoles is 16.1 Å, corresponding to a potassium coverage of 2.7 at. %. The potentials at a lateral distance of 3.2 (K/Rh site) and 6.4 Å (Rh site) from a dipole (thick lines) and the potentials at the positions of the noble gas atoms (dashed line; see also Fig. 8, top curve) are indicated. Above 15 Å from the image plane (surface), the electrostatic potential is virtually homogeneous; a heterogeneous surface potential exists only close to the surface. Hence an adsorbed molecule senses the position of the promoter atom only when it is close to the surface. Further away, adsorbates sense a homogeneously lowered potential, which corresponds to the macroscopic work-function decrease.

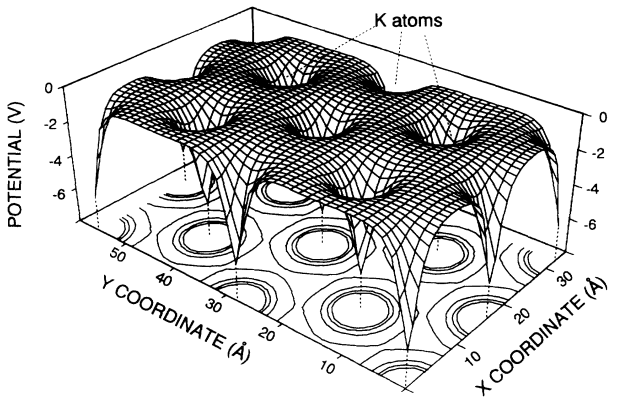

FIG. 10. Map of the potential in a hexagonally ordered network of dipoles at 2.5 Å from the image plane. Parameters as in Fig. 9. The positions of the dipoles (potassium atoms) are indicated by the minima. The equipotential lines for −1.05, −0.84, −0.63, and −0.42 V are indicated in the bottom plane. They are nearly circular close to a potassium atom, indicating that here the potential is mainly determined by the nearest dipole. The equipotential line of, for example, −0.42 V has a clear hexagonal symmetry due to the cumulative influence of all dipoles on the surface. The figure represents the change in effective work function that an adsorbate senses on potassium-promoted Rh(111).

potassium-induced change in effective work function that adsorbates feel when they are adsorbed on a potassium-promoted surface.

V. CONCLUSIONS

The potassium-induced change in local surface potential on potassium-promoted Rh(111) has been estimated by measuring photoemission spectra of adsorbed Xe, Kr, and Ar. The ionization energy for Xe, Kr, and Ar adsorbed on clean Rh(111), found from addition of the binding energy in UPS and the macroscopic work function, is the same as found for these gases on other substrates, indicating that all three gases can be used as a probe for the local surface potential. The trend in extra-atomic relaxation energies for Xe, Kr, and Ar, due to the Rh surface, are in agreement with the relative sizes of the atoms.

The HeI–UPS spectra of submonolayers of Xe, Kr, or Ar adsorbed on potassium-covered Rh(111) reveal at least two different adsorption sites on the surface. This indicates a heterogeneity of the surface potential at these surfaces. The noble gas atoms probe the potential averaged over the valence-p orbital, which in first-order approximation equals the potential at the center of the probe atom. With this assumption we find at all potassium coverages studies (2.7, 4.1, and 5.0 at. %) a strongly decreased surface potential close to a potassium atom (<4 Å), which depends on the distance. Further away (>5 Å) a rather constant potential is found, which is significantly lower than on unpromoted Rh(111). The decrease with respect to unpromoted Rh(111) amounts to −0.4 eV at a potassium coverage of 2.7 at. %,—0.7 eV at 4.1 at. % and −1.0 at 5.0 at. %. All potentials depend on the potassium coverage, but the influence of the potassium coverage on the long-ranged lowering of the potential is larger. The dependence on the potassium coverage indicates that the surface potential on potassium-promoted Rh(111) results from a cumulative effect of all potassium atoms on the surface.

The measured surface potentials are predominantly of electrostatic origin, indicated by the semiquantitative agreement between the calculated electrostatic potential in a network of dipoles and the experimental data. This agreement demonstrates that the presence of dipoles on the surface is enough to cause the observed changes in potential; long-range changes in electronic structure of the substrate surface are not required.

ACKNOWLEDGMENTS

The authors wish to thank Professor R. A. van Santen for discussions. Financial support from the Heinrich Hertz Stiftung and the Netherlands Organization for Scientific Research (NWO) through Grant No. PGS 70-154 is gratefully acknowledged.

*Corresponding author.

[1]G. Ertl, in *Catalysis, Science and Technology,* edited by J. R. Anderson and M. Boudart (Springer-Verlag, Berlin, 1983), Vol. 4, p. 210.

[2]M. E. Dry, in *Catalysis, Science and Technology* (Ref. 1), Vol. 1, p. 159.

[3]M. P. Kiskinova, *Poisoning and Promotion in Catalysis Based on Surface Science Concepts and Experiments,* Studies in Surface Science and Catalysis Vol. 70 (Elsevier, Amsterdam, 1992).

[4]H. P. Bonzel, Surf. Sci. Rep. **8**, 43 (1987).

[5]T. Aruga and Y. Murata, Prog. Surf. Sci. **31**, 61 (1989).

[6]G. R. Castro, H. Busse, U. Schneider, T. Janssens, and K. Wandelt, Phys. Scr. **T41**, 208 (1992).

[7]K. Markert and K. Wandelt, Surf. Sci. **159**, 24 (1985).

[8]K. Wandelt, in *Physics and Chemistry of Alkali Metal Adsorption,* edited by H. P. Bonzel, A. M. Bradshaw, and G. Ertl (Elsevier, Amsterdam, 1989), p. 25.

[9]J. W. Niemantsverdriet, *Spectroscopy in Catalysis, An Introduction* (VCH, Weinheim, 1993).

[10]N. D. Lang, S. Holloway, and J. K. Nørskov, Surf. Sci. **150**, 24 (1985).

[11]S. Holloway, J. K. Nørskov, and N. D. Lang, J. Chem. Soc. Faraday Trans. I **83**, 1935 (1987).

[12]E. Wimmer, C. L. Fu, and A. J. Freeman, Phys. Rev. Lett. **55**, 2618 (1985).

[13]J. E. Crowell and G. A. Somorjai, Appl. Surf. Sci. **19**, 73 (1984).

[14]D. Heskett, Surf. Sci. **199**, 67 (1988).

[15]K. J. Uram, L. Ng, M. Folman, and J. T. Yates, Jr., J. Chem.

Phys. **84**, 2891 (1986).
[16]M. Tüshaus, P. Gardner, and A. M. Bradshaw, Surf. Sci. **286**, 212 (1993).
[17]R. A. de Paola, F. M. Hoffman, D. Heskett, and E. W. Plummer, Phys. Rev. B **35**, 4236 (1987).
[18]G. Pirug and H. P. Bonzel, Surf. Sci. **199**, 371 (1988).
[19]L. J. Whitman and W. Ho, J. Chem. Phys. **83**, 4808 (1985).
[20]J. Rogozik and V. Dose, Surf. Sci. **176**, L847 (1986); V. Dose, J. Rogozik, A. M. Bradshaw, and K. C. Prince, *ibid.* **179**, 90 (1987).
[21]K. Wandelt, in *Thin Metal Films and Gas Chemisorption,* edited by P. Wissman (Elsevier, Amsterdam, 1987), p. 268.
[22]K. Wandelt, in *Chemistry and Physics of Solid Surfaces VIII,* edited by R. Vanselow and R. Howe, Springer Series in Surface Sciences Vol. 22 (Springer, Berlin, 1991), p. 289.
[23]T. V. W. Janssens, J. W. Niemantsverdriet, and R. A. van Santen, J. Chem. Phys. (to be published).
[24]T. V. W. Janssens, K. Wandelt, and J. W. Niemantsverdriet, Catal. Lett. **19**, 263 (1993).
[25]K. Wandelt, S. Daiser, R. Miranda, and H.-J. Forth, J. Phys. E **17**, 22 (1984).
[26]J. W. Niemantsverdriet and K. Wandelt, J. Vac Sci. Technol. A **7**, 1742 (1989).
[27]R. D. B. Fraser and E. Suzuki, Anal. Chem. **41**, 37 (1969).
[28]D. W. Turner, C. Baker, D. A. Baker, and C. R. Brundle, *Molecular Photoelectron Spectroscopy* (Wiley Interscience, New York, 1970).
[29]U. Schneider (private communication).
[30]D. R. Mullins, J. M. White, and H. S. Luftman, Surf. Sci. **167**, 39 (1986).
[31]K. Kalki (private communication).
[32]N. W. Ashcroft and N. D. Mermin, *Solid State Physics* (Holt-Saunders, Philadelphia, 1976), pp. 391 and 401.
[33]H. Ishida, Phys. Rev. B **38**, 8006 (1988).
[34]N. D. Lang and A. R. Williams, Phys. Rev. B **18**, 616 (1978).